Sputtering Thresholds*

D. E. HARRISON, JR.,† AND G. D. MAGNUSON
Physics Section, Convair, San Diego, California
(Received January 27, 1961)

We attempt to give a logically coherent definition of the term "sputtering threshold," and establish criteria which may determine an experimental threshold. The Silsbee chain mechanism and the experimentally observed preferred direction of emission from single crystals are used to establish a threshold theory. Two models are required, one generally applicable when the mass ratio is less than one, and another when it is greater than one. Single-crystal threshold laws are obtained, and polycrystalline laws follow for face-centered cubic crystals by averaging the single-crystal forms. An approximate technique for the evaluation of surface atomic binding energies is presented so that the thresholds can be compared with experimental results. In all cases the theoretical thresholds are less than or comparable to experimental "thresholds."

INTRODUCTION

RECENTLY reported attempts to measure sputtering thresholds by Morgulis and Tishchenko,[1] Wehner and Stuart,[2] and McKeown[3] depend upon experimental techniques which have reached a high degree of sophistication. This effort seems to warrant rather careful theoretical analysis to attach meaning to the term "sputtering threshold," and a discussion of what may be expected from threshold measurements. Some questions are raised which can only be answered by further experimentation. We extend the Silsbee chain mechanism[4] as developed by Leibfried,[5] present a new theory of the single-crystal sputtering threshold, and treat the polycrystalline threshold problem.

SUBLIMATION, EVAPORATION, AND SPUTTERING

During the last decade a series of experiments has lead to successively lower reported values for the "sputtering threshold." Thresholds have been reduced from the 50- to 300-ev range reported by Wehner[6] to the recently reported values in the 5- to 15-ev range. As these energies approach the corresponding heats of sublimation, we must inquire whether a sputtering threshold really exists, or whether threshold measurements are actually chasing a will-of-the-wisp. To answer this question, we consider the sublimation process in some detail.

Suppose we begin with a perfect crystal at absolute zero. As soon as the temperature is raised above 0°K, defects begin to form, and the statistical probability exists that some surface atom will acquire sufficient energy to break away from the surface, i.e., the crystal now has a vapor pressure.

Historically, we have always thought of the sublimation process as a purely surface phenomenon, but the Silsbee chain mechanism forces us to re-examine the analysis. In brief, the Silsbee mechanism shows that if by means of a statistical fluctuation a lattice atom acquires energy and momentum in one of the close-packed directions of the lattice, the energy will propagate along the close-packed "chain" for a considerable distance. Applied to the sublimation problem, this mechanism seems to indicate that in a more general sense sublimation may be initiated well below the metal surface by the formation of a high-energy atom, which then transmits that energy to a surface atom along a chain. In all cases it is the surface atom which "sublimes." This approach suggests that the sublimation rate will be a volume effect rather than a surface effect. Evaporation from a liquid surface should be a much simpler process, because there is no evidence that the chaining mechanism will operate in a liquid.

At temperatures well below the normal melting point, we expect to find that high-vacuum sublimation exhibits the characteristic spot patterns of single-crystal sputtering. Yurasova[7] unsuccessfully attempted to find such a pattern in copper. However, this experiment does not invalidate the mechanism, because it was conducted at 950°C, which is very close to the normal melting point of copper. At such temperatures the defect density near the surface will be very large, perhaps approaching the "liquid surface layer" model suggested by Gurney.[8] These defects will effectively disrupt the close-packed chain structure near the surface and lead to liquid-like sublimation near the melting point. Evidence supporting this model has been published by Bol'shov.[9] At temperatures well below the melting point, we may expect the characteristic spot pattern superimposed upon a uniform cosine "haze" produced by the liquid-type "surface sublimation." Although it might well require a millenium to complete, a sublimation spot-pattern experiment on copper (run near room tem-

* This work was supported by Air Force Cambridge Research Center contract.
† Permanent address: University of Toledo, Toledo, Ohio.
[1] N. D. Morgulis and V. D. Tishchenko, (a) Soviet Phys.—JETP **3**, 52 (1956); (b) Bull. Acad. Sci. USSR, Phys. Ser. **20**, 10, 1082 (1956).
[2] R. V. Stuart and G. K. Wehner, Phys. Rev. Letters **4**, 409 (1960).
[3] D. McKeown, Bull. Am. Phys. Soc. **5**, 286 (1960).
[4] R. H. Silsbee, J. Appl. Phys. **28**, 1246 (1957).
[5] G. Leibfried, J. Appl. Phys. **30**, 1388 (1959).
[6] G. K. Wehner, Phys. Rev. **102**, 690 (1956).
[7] V. E. Yurasova, Soviet Phys.—Tech. Phys. **3**, 1806 (1958).
[8] C. Gurney, Proc. Phys. Soc. (London) **A62**, 639 (1949).
[9] V. G. Bol'shov, Bull. Acad. Sci. USSR, Phys. Ser. **20**, 10, 1020 (1956).

perature, where most sputtering experiments are performed) would be very instructive. Experiments in the range 600–700°C appear more practical and may exhibit the effect. If the bulk sublimation effect does exist, it might be detectable as a change in vapor pressure across a solid phase change in a metal or alloy.

Suppose we now add the additional complication of ion bombardment. We expect at least three noticeable effects:

1. It will raise the crystal temperature. The effect can be controlled by decreasing the bombardment intensity, at the expense of total yield. Cooling the target will help, but only if the temperature gradient across the target can be kept small.
2. Ion bombardment will increase the "surface" defect density, which tends to decrease the mean surface binding energy, but for experiments run at room temperature many of the defects will be self-annealing. The resulting surface structure approximates the basic crystal fairly closely in most cases, but Wehner[10] has some evidence that bombardment tends to rearrange the diamond-type lattice of germanium into body-centered cubic (bcc).
3. Finally, if the ions are sufficiently energetic, they initiate mechanical sputtering. Here, mechanical sputtering refers to a momentum-energy exchange mechanism which frees the end member of a close-packed chain. Our ignorance of true surface conditions suggests that this bulk material approach will ultimately be more fruitful than a detailed examination of Henschke's "single-collision mechanism."[11] Experimentally, we can hope to establish a "spot-pattern threshold," i.e., an energy at which the patterns first appear after some reasonable period of time.

Because sublimation effects must inevitably obscure the threshold for large angles of incidence and for sputtering from preferred surface positions, it appears that the sputtering threshold is a meaningless concept, except in the single-crystal case. Perhaps, on monocrystals, the appearance of spots will define a relatively sharp threshold. We shall assume that this threshold is detectable, and derive a theory of its dependence upon ion energy and angle of incidence.

Because of the high density of defects near the surface, there probably is little correlation between sputtering thresholds and the displacement energy needed for radiation damage studies. A more promising approach would be a correlation between angles of emission and the variation of cross sections with energy. Wehner[10] is just beginning to obtain the data required for these studies. The researches of Gillam[12] indicate that sputtering measurements may also produce useful information about the range of heavy particles in metals at low energies.

[10] G. K. Wehner, General Mills Rept. No. 1930, February, 1960 (unpublished).
[11] E. B. Henschke, Phys. Rev. **106**, 737 (1957).
[12] E. Gillam, J. Phys. Chem. Solids **11**, 55 (1959).

ENERGY TRANSPORT BY CHAINS

The original suggestion of energy transport by close-packed chains was made by Silsbee.[4] His analysis was considerably extended by Leibfried,[5] who made a study of the effect of a chaining mechanism upon radiation damage. The first part of this section is a somewhat shortened recapitulation of the Leibfried presentation, which should be consulted for details.

Chains without Dissipation

We consider a collision between two hard-sphere atoms of radius r_H, where $r_H=\frac{1}{2}R$, R being the distance of closest approach upon collision. The interaction distance R may be determined from the relation $E=2V(R)$, where E is the kinetic energy of the moving atom, and $V(R)$ is the interaction potential between pairs of atoms. Let D be the distance between atomic centers in the chaining direction.

Consider the nth member of a chain, with energy E_n, which moves in the θ_n direction (see Fig. 1). From simple geometry, we obtain

$$\sin\theta_{n+1}=\sin\theta_n[\alpha\cos\theta_n-(1-\alpha^2\sin^2\theta_n)^{\frac{1}{2}}], \tag{1}$$

where $\alpha=D/R$, and conservation of energy and momentum require that

$$E_{n+1}=E_n(1-\alpha^2\sin^2\theta_n). \tag{2}$$

If $\theta_{n+1}<\theta_n$, part of the energy will be focused along the chain, with the result that energy is transported for many atomic diameters. From Eq. (1) we readily establish that the maximum focusing angle is determined by $\cos\theta_F=\alpha/2$, which is equivalent to the requirement that $D\leq 2R$. We shall be interested in energy ranges where $\alpha\simeq 2$; therefore, if we set $\alpha=2-\eta$, the limiting angle may be expressed as $\sin^2\theta_F=\eta$, where we have assumed $\eta^2/4\ll 1$, i.e., $\eta\leq 0.2$. In our work we make the somewhat more restrictive approximation that $\sin^2\theta_n=\theta_n^2=\eta$. Upon substituting $\alpha=2-\eta$, and by using the small-angle approximation, Eq. (1) becomes

$$\theta_{n+1}=\theta_n[1-\eta+\theta_n^2]. \tag{3}$$

Now if $\theta_{n+1}-\theta_n$ is small, we can write

$$\theta_{n+1}=\theta_n+(d\theta_n/dn)(1),$$

and Eq. (3) is reduced to the differential equation

$$d\theta_n/dn=(-\eta+\theta^2)\theta. \tag{4}$$

We have tacitly assumed that n may become large; therefore, the differential equation is a fair approximation to the difference equation. Upon integration, we obtain

$$\int_{\theta_0}^{\theta_n}\frac{d\theta}{\theta(\theta^2-\eta)}=n,$$

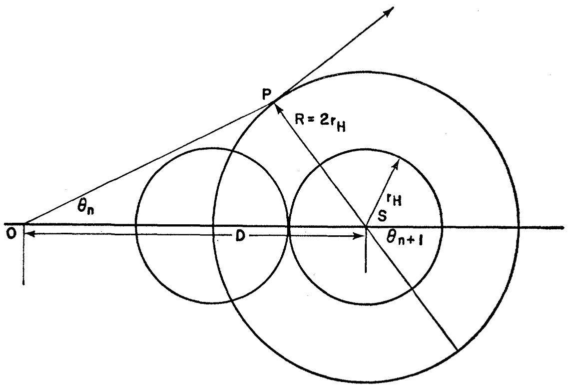

FIG. 1. This figure shows the dynamic variables in a single collision process. For clarity it is drawn with $D>2R$; i.e., for the case where chaining cannot occur.

and after some algebra,

$$\theta_n^2=\frac{-\eta e^{-2\eta n}}{(1-e^{-2\eta n}-\eta/\theta_0^2)}. \tag{5}$$

For later use it will be convenient to define

$$x_n=(1-e^{-2\eta n}-\eta/\theta_0^2)$$

and

$$x_0=-\eta/\theta_0^2. \tag{6}$$

After following the same type of manipulation, a differential equation which governs the energy transport to the nth atom is obtained:

$$dE/dn=-4(1-\eta)\theta_n^2E.$$

Again integrating, we find

$$E_n=E_0[1-(\theta_0^2/\eta)(1-e^{-2\eta n})]^{2(1-\eta)}, \tag{7}$$

where E_0 is the original energy, and θ_0 the original direction of the first member of the chain. Usually $\eta\ll1$. Note that in this special case there is an asymptotic energy $E_\infty=E_0(1-\theta_0^2/\eta)^2$ which will continue down the chain indefinitely. Such a transport mechanism will operate until the chain is interrupted by a vacancy, dislocation, or impurity atom.

For chains produced by collisions in real crystals, the angle θ_0 is unknown. However, we can obtain the probability of any given E_∞:

$$f(E_\infty)=\tfrac{1}{2}[1/(E_0E_\infty)^{\frac{1}{2}}],$$

and average to obtain the mean E_∞:

$$\bar{E}_\infty=E_0/3.$$

Chains with Dissipation

We now re-examine the chain problem on the assumption that between each collision some small fraction of the particle energy is lost to the surrounding lattice atoms. Equation (1) is not modified, but Eq. (2) becomes

$$E_{n+1}=E_n(1-\epsilon)(1-\alpha^2\sin^2\theta_n). \tag{8}$$

The θ_n analysis is unchanged, but the energy analysis is more complicated. After manipulation, the energy differential equation becomes

$$dE/dn=-(4\beta\theta_n^2+\epsilon)E, \tag{9a}$$

where we have set $\beta=(1-\eta)(1-\epsilon)$.

This equation is more conveniently written with x as the independent variable,

$$\frac{dE}{E}=2\beta\frac{dx}{x}-\frac{\epsilon}{2\eta}\frac{dx}{(1-\eta/\theta_0^2-x)}. \tag{9b}$$

The integration is now straightforward, and we finally obtain

$$E_n=E_0e^{-\epsilon n}[1-(\theta_0^2/\eta)(1-e^{-2\eta n})]^{2\beta}. \tag{10}$$

In the sputtering threshold work we shall be interested only in cases where η is very small. To this approximation we find that

$$E_n=E_0e^{-\epsilon n}[1-2\theta_0^2n]^{2\beta}, \tag{11}$$

and ϵ completely dominates the energy loss mechanism. It is a straightforward but rather messy calculation to obtain the average energy after n collisions. Finally, we find

$$\bar{E}_n=\left(\frac{1}{2\beta+1}\right)\left(\frac{1-\exp[-2\eta n(1+2\beta)]}{1-\exp(-2\eta n)}\right)E_0e^{-\epsilon n}, \tag{12}$$

and again the lattice loss mechanism is dominant.

Unfortunately, there are no direct measurements of chain losses available at the present time. Calculations by Vineyard *et al.*[13] indicate that lattice losses per collision are fairly small, perhaps only a few percent of the atom's energy. These results seem to favor a constant-loss mechanism, rather than the constant fractional loss used in this analysis. The constant-loss mechanism leads to a discontinuous function for E_n which is not particularly amenable to calculation. Silsbee,[4] using analytic procedures, plots a more complicated energy dependence for the loss function. In the absence of a definitive experiment we accept the Leibfried mechanism,[5] the general results of the preceding analysis, and assume that $\epsilon<0.05$.

THEORY OF THE SPUTTERING THRESHOLD

All low-energy sputtering experiments performed on single crystals exhibit preferential sputtering in directions approximating the close-packed directions of the crystal. The resulting spot patterns persist to the lowest bombardment energies. We use this preferred emission direction to provide a basis for a theory of the

[13] G. H. Vineyard, J. B. Gibson, A. N. Goland, and M. Milgram, Bull. Am. Phys. Soc. 5, 26 (1960); G. H. Vineyard, *ibid.*, p. 175.

sputtering threshold as defined previously. The dependence upon preferential sputtering distinguishes this theory from the work of Henschke[11] and Langberg.[14] We shall see that the chain mechanism produces a more tractable theory of the sputtering threshold.

In much of the succeeding work we shall make reference to "chain," or "chain direction" where the term "close-packed direction" might be more appropriate. Furthermore, a chain may consist of only *two* atoms, although in some instances it will be considerably longer. These semantic liberties will simplify presentation of the material.

A threshold theory based upon the Silsbee effect will be independent of the surface configuration so long as the surface is clean. Surface irregularities should neither enhance nor defeat the mechanism, although they will certainly affect the surface binding energy, and hence numerical values obtained from the theory. A high density of defects may change the close-packed directions from those characteristic of the underlying crystal, but near room temperature some sort of close-packing must exist. Defects would disrupt long-chain effects, initiated far below the surface, but near threshold these effects are not energetically possible. It will be convenient to think of chains consisting of two or three atoms, although ten-member chains are plausible at the energies under consideration, but because a maximum efficiency mechanism is required at threshold, chains inevitably will be quite short. Again, efficiency considerations suggest that we examine only those cases in which energy is transmitted exactly in the chain direction. Thus, we set $\theta \simeq 0$. As n is to be small, we may take $e^{-n\epsilon} \simeq 1$ and as a first approximation consider a loss-free mechanism. We shall see that dissipation effects would be fairly simple to include, but that $\theta_0 \neq 0$ introduces larger complications.

Still another general consideration is that, regardless of the bombarding ion, a surface atom requires a certain energy to sputter. This binding energy will depend upon the surface temperature, the defect state of the surface, and the position of the atom on the surface. We expect this energy to be considerably less than the macroscopic heat of sublimation. For numerical work, we write H_{hkl}, but the only experimental data refer to polycrystalline samples.

We assume that the end member of a chain is sputtered. At this stage we have made two requirements upon the particle which delivers the sputtering energy to the chain: It must deliver H_{hkl}, and *it must be moving in the chain direction* so that it can make a maximum efficiency energy transfer to the chain. We write $H_{hkl} = T_m E_A$, where $T_m = 4\mu/(1+\mu)^2$, and $\mu = m_{\text{ion}}/m_{\text{atom}}$, the mass ratio. To deal with a dissipative medium, replace H_{hkl} by $H_{hkl}\exp(\epsilon\bar{n})$, where $\bar{n}$ is the mean-chain length.

The following effects influence the production of a

[14] E. Langberg, Phys. Rev. **111**, 91 (1958).

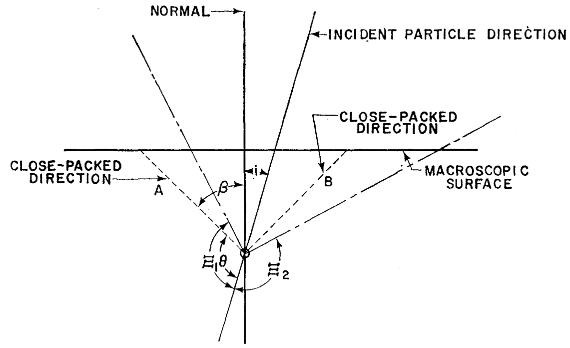

FIG. 2. Illustration of the angles involved in the averaging process and the relation between the three angles used in the polycrystalline section of the manuscript.

particle A with the requisite energy and direction of motion.

Angular Considerations

For a given angle of incidence i, a reorientation angle θ will be required (Fig. 2). Two effects limit the possible scattering angles θ_n for the two-body interactions which ultimately produce the angle θ.

The mass ratio places limitations upon the maximum value $\theta_{\max}$ of θ_n. From collision kinetics we have

$$\tan\theta_n = (\sin\vartheta_n)/(\mu + \cos\vartheta_n), \tag{13}$$

where θ_n is measured in the laboratory system (lab) and ϑ_n is the center-of-mass system (c.m.) scattering angle. By differentiation, we find that $\cos\vartheta_{\max} = -1/\mu$ which is obviously a real restriction for $\mu \geq 1$. When substituted into Eq. (13), the condition gives $\tan\theta_{\max} = (\mu^2 - 1)^{-\frac{1}{2}}$. The graph of this function appears in Fig. 3.

The crystal lattice sets a limiting minimum scattering angle, in the sense that a maximum impact parameter exists. All impacts which exceed the maximum parameter are actually smaller angle impacts upon another atom. If for the face-centered cubic (fcc) crystal we assume equal radii for bullet and target atoms, the maximum impact parameter is $(1/\sqrt{2})D$. The resulting minimum scattering angles are also shown in Fig. 3. This method of establishing the minimum scattering angles contains two obvious sources of error: The atom size (cross section) depends on the energy; therefore, larger impact parameters are possible at higher energies; and, of course, the incident ion need not have the same radius as a lattice atom. Both of these effects will usually reduce the minimum scattering angle.

Careful examination of Fig. 3 is very instructive. We first note that for $\mu > 1$ the range of possible scattering angles is very restricted, while for $\mu < 1$, the range is quite large. This examination suggests that for $\mu < 1$ it will be convenient to reorient the incident ion, while for $\mu \geq 1$ we should look for another mechanism.

Energy Considerations

The minimum scattering angle has a profound effect upon the scattering mechanism because it sets an upper limit upon the factor

$$r_n = 1 - T_m \sin^2(\vartheta_n/2), \qquad (14)$$

where $r_n = E_n/E$ measures the fraction of energy retained by the bullet after a collision. Suppose we compare the effect of n equal small-angle collisions such that $\vartheta_n = \vartheta/n$. If n is large we may find that the combined retention of n such collisions, $R_n = (r_n)^n = [1 - T_m \sin^2(\vartheta_n/2)]^n$ will be greater than R_1. The minimum angle limitation shows that if the reorientation is to be 50 deg, for example, we need not consider the possibility of ten 5-deg collisions, although it may be pertinent to consider the possibility of two 25-deg scatterings as well as the single 50-deg interaction. When $n > 1$, we need consider only the case of n *equal angle* interactions, for it will always give a retention factor greater than a combination of n arbitrary angles. That is, $[1 - T_m \sin^2(\vartheta_n/2)]^n = (1-t_n)^n > \prod_j^n (1-t_j)$, where $t_n = 1 - r_n$, $t_j = t_n + a_j$, the a_j may be positive or negative, and $\sum_j^n a_j = 0$.

We observe that if the incident particle has an energy E_0 in the beam, it will have an energy $E_A = E_0 R_n$ when it has finally been reoriented into the chain direction. For any particular case, we may have to examine more than one value of n to determine which will maximize R_n. The minimum angle condition indicates that we may use R_1 whenever the mass ratio is small, and it is a reasonable first approximation whenever $\mu < 1$.

Mechanism I. $\mu < 1$

By combining the preceding results, we obtain

$$H_{hkl} = R_n T_m E_0,$$

and the threshold energy may be written

$$E_{tn}^{<} = (H_{hkl}/T_m) r_n^{-n}, \qquad (15)$$

where ϑ_n measured in the c.m. system corresponds to θ/n in the lab system. Usually we may set $n = 1$, so that

$$E_{t1}^{<} = (H_{hkl}/T_m)[1 - T_m \sin^2(\vartheta/2)]^{-1}. \qquad (16)$$

Equation (15) was derived on the assumption that the original incident particle is reoriented into the chain direction. An alternative mechanism is possible if we assume that E_A is delivered to the chain by a moving lattice atom, rather than by the incident particle. If we assume that maximum energy is transferred to a lattice atom in the first collision, that atom will receive an energy $E_1 = T_m E_0$. From this point on, the remaining n collisions all occur between identical particles, so that $r_n' = 1 - \sin^2(\vartheta_n/2) = \cos^2(\vartheta_n/2)$. Now $T_m \leq 1$, so that $r_n' < r_n$ and this process is less efficient than the mechanism leading to Eq. (15).

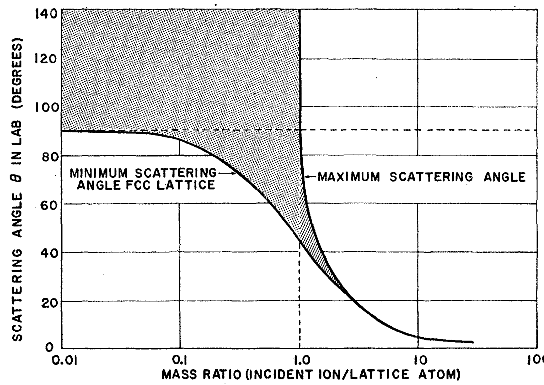

FIG. 3. From this figure we can see how considerations of energy transfer and lattice spacing limit the allowable scattering mechanisms. The maximum scattering angle curve is exact. Note that it terminates at 90° when $\mu = 1$. The minimum scattering angle is approximate. See the body of the paper for a discussion of its validity.

Because of the relation $\theta_n + \psi_n = \pi/2$, which applies when the masses are equal, as well as the identical nature of the colliding particles, it is apparent that E_n', the energy transferred to the nth lattice atom, is given by

$$E_n' = E_1 \sin^{2n}\theta_n = E_1 \cos^{2n}\psi_n,$$

where ψ_n is the recoil angle (lab), so that

$$T_n = t_n{}^n = \cos^{2n}\psi_n,$$

which is just $R_n = r_n{}^n$. We conclude that the alternative mechanism gives the same results whether one atom is assumed to make n collisions terminating at the chain, or n atoms make collisions so that the final recoil has the proper termination at the chain.

Mechanism II. $\mu \geq 1$

When the mass ratio is greater than unity, angular considerations restrict the possible scattering angles so much that the mechanism leading to Eq. (15) cannot usually operate. When $\mu \simeq 1$ it may be appropriate to consider this possibility, but in most cases we must fall back upon the alternative mechanism which leads to

$$E_{tn}^{>} = (H_{hkl}/T_m) \sec^{2n}(\vartheta_n/2). \qquad (17)$$

Except at very large angles of incidence, at least two collisions will be required to scatter the moving lattice atom into the chain direction. Now for equal-mass collisions, $\theta = \vartheta/2$, so that setting $\theta_n = \theta/n$ we obtain

$$E_{tn}^{>} = (H_{hkl}/T_m) \sec^{2n}\theta_n. \qquad (18)$$

When $\mu \neq 1$, i.e., for use in the $\mu < 1$ case,

$$\sin^2(\tfrac{1}{2}\vartheta) = \tfrac{1}{2}\{1 + \mu \sin^2\theta - \cos\theta(1 - \mu^2 \sin^2\theta)^{\frac{1}{2}}\}; \quad (19)$$

so that we have from Eq. (15),

$$E_{tn}^{<}=H_{hkl}\Phi_{tn}^{<},$$
$$\Phi_{tn}^{<}=(1/T_m)\{1-\tfrac{1}{2}T_m[1+\mu\sin^2\theta_n-\cos\theta_n(1-\mu^2\sin^2\theta_n)^{\frac{1}{2}}]\}^{-n}. \quad (20)$$

Upon collecting results, the two simplest cases give, for mass ratio greater than unity,

$$E_{t2}^{>}=\frac{H_{hkl}}{T_m}\sec^4(\tfrac{1}{2}\theta)=\frac{H_{hkl}}{T_m}\frac{4}{(1+\cos\theta)^2}, \quad (21)$$

and, for mass ratio less than unity,

$$E_{t1}^{<}=\frac{H_{hkl}}{T_m}\{1-\tfrac{1}{2}T_m[1+\mu\sin^2\theta-\cos\theta(1-\mu^2\sin^2\theta)^{\frac{1}{2}}]\}^{-1}. \quad (22)$$

For the remainder of the work we shall consider only these two threshold laws.

Single-Crystal Thresholds

We may immediately obtain expressions for the sputtering threshold as a function of angle of incidence upon the fcc lattice by determining the angle β which is appropriate for the specified crystal plane. In cases where more than one possibility exists, we chose the value of β which requires the smallest value of θ. With this restriction,

$$\beta_{100}=45°,$$
$$\beta_{110}=60°,$$
$$\beta_{111}=35.26°,$$

and, in general, $\theta=\pi-(\beta+i)$. When these values are substituted into Eqs. (21) and (22) we have

$$E_{t2}^{>}=(H_{hkl}/T_m)(4/\{[1-\cos(\beta+i)]^2\}, \quad (23)$$

and

$$E_{t1}^{<}=H_{hkl}\Phi_{t1}^{<}. \quad (24)$$

We note that the factor $\Phi_{t2}^{>}(\beta,i)=4/[1-\cos(\beta+i)]^2$, which occurs when $\mu\geq 1$, is independent of μ. Thus, the variation of threshold with angle should have the same form for all mass ratio greater than 2.5, (see Fig. 3), and a general law will probably be valid over the entire mass ratio range greater than one. The factor $\Phi_{t2}^{>}(\beta,i)$ is exhibited in Fig. 4 for the three values of β appropriate for the fcc lattice.

The corresponding factor,

$$\Phi_{t1}^{<}(\beta,i,\mu)=(1/T_m)\{1-\tfrac{1}{2}T_m[1+\mu\sin^2(\beta+i)+\cos(\beta+i)[1-\mu^2\sin^2(\beta+i)]^{\frac{1}{2}}]\}^{-1},$$

appears in Fig. 5 for two mass ratios which are currently of experimental interest. Figure 6 shows the variation

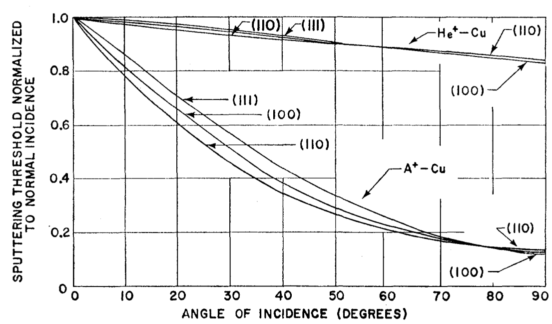

FIG. 5. Here we have plotted angular dependences of the single-crystal threshold for two systems which represent extremes of the mass ratio. We note that there is little crystal orientation effect for small mass ratios, but that orientation effects become quite pronounced when the mass ratio approaches unity.

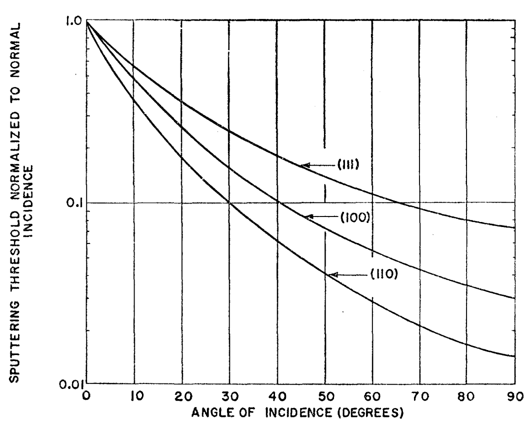

FIG. 4. A single curve is sufficient to describe the angular dependence of the sputtering ratio on a single crystal for all $\mu>1$. By actual computation we find that the second mechanism leads to lower thresholds than the first for all mass ratios greater than $\sim$0.7; so that the curves are valid for $\mu>\sim 0.7$. We have not determined whether an $n=2$ first mechanism will lead to still lower thresholds. Although the method of presentation obscures the dependence, the normal incidence thresholds are strong functions of the crystal orientation. Thus for (110), $\Phi_{t2}^{>}(60°,0°)=16.0$, for (100), $\Phi_{t2}^{>}(45°,0°)=46.6$, and for (111), $\Phi_{t2}^{>}(35.26°,0°)=119$.

of $\Phi_1^{<}(\beta,0,\mu)$ as a function of μ for the three values of β appropriate for the fcc lattice. For comparison, two of the second-mechanism curves are included. The third falls off scale. Apparently, the second mechanism will lead to a lower threshold than the first as μ approaches one.

Equations (23) and (24) suggest that when $i\neq 0$ anisotropies should exist in the thresholds for different portions of the spot pattern. For example, on the (110) surface of a fcc crystal these equations predict one threshold for the "far" spots, and another for the "near" spots if the crystal is oriented so that the [100] directions in the surface are either perpendicular or parallel to the projection of the beam upon the surface. This anisotropy should continue to higher energies, until statistical processes begin to control the activation of chains. At the present time, only high-energy data seem to be available; in this connection, see Yurasova, Pleshivtsev, and Orfanov,[15] who report isotropic

[15] V. E. Yurasova, N. V. Pleshivtsev, and I. V. Orfanov, Soviet Phys.—Tech. Phys. 37, 689 (1960).

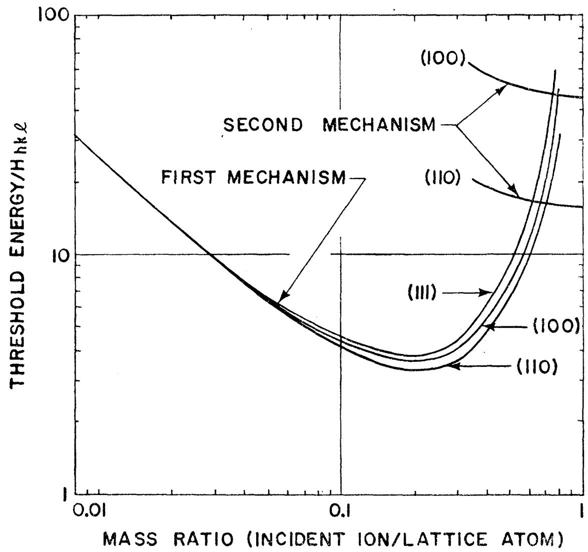

FIG. 6. Here we show the dependence of the factor $\Phi^{<}(\beta,0,\mu)$ upon the mass ratio. We note that the second mechanism is actually more efficient than the first for $\mu>\sim 0.7$; see the restriction in the caption of Fig. 5. We may obtain single-crystal sputtering thresholds at normal incidence by multiplying H_{hkl} times a value read from this curve.

patterns in the 10- to 40-kev range for argon sputtering single-crystal copper at large angles of incidence, and Rol,[16] who reports angular dependences which are independent of the angle of incidence.

POLYCRYSTALLINE THRESHOLDS

The results of the previous section are of considerable theoretical interest, but they are not directly applicable to the presently available experimental data. Here we shall use a rather rough approximation technique to calculate polycrystalline sputtering thresholds.

If we assume that there are no preferred orientations in the polycrystalline sample, we can average the single-crystal threshold expressions over all allowable angles θ. That is, we are comparing the result of an average over all angles, with the experimental average of single-crystal data over all crystal orientations. The results should be at least approximately comparable.

During the process of integration, we must be very careful that we always deal with the smallest possible reorientation angle θ. An examination of Fig. 2 will indicate that when $0\leq i\leq \pi/4$ we must change close-packed directions in mid-integration, while when $\pi/4\leq i\leq\pi/2$, one close-packed direction is sufficient. As a concrete example, suppose we consider close-packed directions which make an angle of 45° with the normal. Using Fig. 2, think of the normal line and line of incidence as fixed, and allow the surface and close-packed directions to rotate about 0. Then so long as A lies in the range Ξ_1, there is a minimum reorientation to reach chain A. However, as soon as A moves outside of Ξ_1, the minimum reorientation will be to chain B, and θ will lie in Ξ_2. Expressed analytically, when $0\leq i\leq\pi/4$ we integrate $\pi/2-i\leq\theta\leq 3\pi/4$, and then *subtract* the integral of θ in the range $3\pi/4\geq\theta\geq\pi/2+i$. When $\pi/4\leq i\leq\pi/2$ this difficulty does not occur, because A never moves out of the range Ξ_1. All possible orientations are included if the crystal is also rotated about the normal, but this motion does not affect the average, because close-packed directions describe cones about the normal. The method of averaging is valid only when the close-packed directions are mutually perpendicular.

[16] P. K. Rol, Dissertation, Amsterdam (1960). One of the authors (DEH) would like to record an extended and very rewarding correspondence with Dr. Rol which has contributed greatly to his studies of sputtering.

Threshold for $\mu\geq 1$

Case A. $\pi/4\leq i\leq\pi/2$

For this case, we perform a straightforward average of $\Phi_{t2}^{>}(\theta)$ over the range $\frac{1}{2}\pi-i\leq\theta\leq\pi-i$,

$$\int_{\frac{1}{2}\pi-i}^{\pi-1}\sec^4(\tfrac{1}{2}\theta)d\theta=2\left\{\frac{1}{3}\cot^3\left(\frac{i}{2}\right)+\cot\left(\frac{i}{2}\right)-\frac{1}{3}\left[\frac{1-\tan(\frac{1}{2}i)}{1+\tan(\frac{1}{2}i)}\right]^3-\left[\frac{1-\tan(\frac{1}{2}i)}{1+\tan(\frac{1}{2}i)}\right]\right\},$$

and

$$\bar{E}_L^{>}(i)=\frac{4}{\pi}\frac{H_{hkl}}{T_m}\left\{\frac{1}{3}\cot^3\left(\frac{i}{2}\right)+\cot\left(\frac{i}{2}\right)-\frac{1}{3}\left[\frac{1-\tan(\frac{1}{2}i)}{1+\tan(\frac{1}{2}i)}\right]^3-\left[\frac{1-\tan(\frac{1}{2}i)}{1+\tan(\frac{1}{2}i)}\right]\right\}\qquad(25)$$

is the large-angle polycrystalline threshold law when $\mu\geq 1$.

Case B. $0\leq i\leq\pi/4$

Here we evaluate the integral

$$\int_{\frac{1}{2}\pi-i}^{\frac{3}{4}\pi}\sec^4(\tfrac{1}{2}\theta)d\theta+\int_{\frac{1}{2}\pi+i}^{\frac{3}{4}\pi}\sec^4(\tfrac{1}{2}\theta)d\theta,$$

and obtain

$$\bar{E}_S^{>}(i)=\frac{4}{\pi}\frac{H_{hkl}}{T_m}\left\{2\left[\frac{1}{3}\tan^3\left(\frac{3\pi}{8}\right)+\tan\left(\frac{3\pi}{8}\right)\right]-\frac{1}{3}\left[\frac{1-\tan(\frac{1}{2}i)}{1+\tan(\frac{1}{2}i)}\right]^3-\frac{1}{3}\left[\frac{1+\tan(\frac{1}{2}i)}{1-\tan(\frac{1}{2}i)}\right]^3-\left[\frac{1+\tan(\frac{1}{2}i)}{1-\tan(\frac{1}{2}i)}+\frac{1-\tan(\frac{1}{2}i)}{1+\tan(\frac{1}{2}i)}\right]\right\}\qquad(26)$$

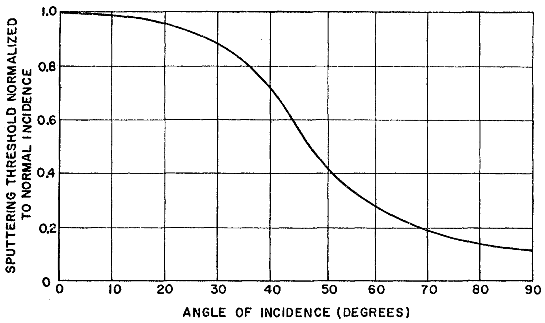

FIG. 7. Polycrystalline threshold values of fcc metals vs angle of incidence for mass ratios >1. The results are normalized to the threshold at 0° angle of incidence.

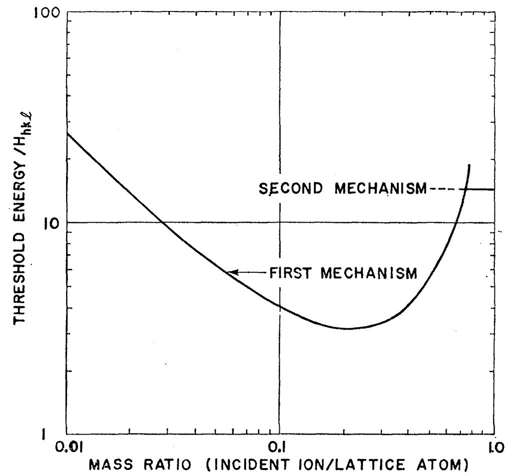

FIG. 9. A plot of E_t/H_{hkl} for mass ratios <1 at normal incidence.

for the small-angle polycrystalline threshold when $\mu \geq 1$. The ratio $\bar{E}^{>}(i)/\bar{E}^{>}(0)$ is plotted in Fig. 7.

Threshold for $\mu<1$

We follow exactly the same procedure when $\mu<1$, but the analysis is much more complicated because now there is no simple relation between ϑ and θ. From Eq. (13) we obtain

$$d\theta=\frac{1}{2\mu}\left[\frac{\mu\cos\vartheta+1}{[(\mu^2+1)/2\mu]+\cos\vartheta}\right]d\vartheta, \tag{27}$$

so that we may write the integral required for averaging as

$$\int_{\theta_0}^{\theta_1}\frac{d\theta}{[1-T_m\sin^2(\vartheta/2)]}=\frac{1}{\mu T_m}\int_{\theta_0}^{\theta_1}\frac{1+\mu\cos\vartheta}{\{[(\mu^2+1)/2\mu]+\cos\vartheta\}^2}d\vartheta. \tag{28}$$

Now the indefinite integral of Eq. (28) is a standard form (Pierce, *Table of Integrals*, No. 306). Upon setting

$$I(x)=\int[1-T_m\sin^2(\tfrac{1}{2}\vartheta)]^{-1}d\theta,$$

we find after manipulation that

$$I(x)=\frac{1}{(1-\mu)^2}\left\{-\frac{(1-\mu^2)}{2}\left[\frac{\sin x}{[(\mu^2+1)/2\mu]+\cos x}\right]+2\tan^{-1}\left[\left(\frac{1-\mu}{1+\mu}\right)\tan(\tfrac{1}{2}x)\right]\right\}, \tag{29}$$

where x corresponds to ϑ evaluated for a particular value of θ through Eq. (19). By using Eq. (19) we find that

$$\cos x=-\mu\sin^2\theta+\cos\theta(1-\mu^2\sin^2\theta)^{\frac{1}{2}}, \tag{30a}$$

$$\sin x=\sin\theta[\mu\cos\theta+(1-\mu^2\sin^2\theta)^{\frac{1}{2}}], \tag{30b}$$

and

$$\tan(\tfrac{1}{2}x)=\frac{1+\mu\sin^2\theta-\cos\theta-(1-\mu^2\sin^2\theta)^{\frac{1}{2}}}{\sin\theta[\mu\cos\theta+(1-\mu^2\sin^2\theta)^{\frac{1}{2}}]}. \tag{30c}$$

Now let

$\theta_1=\frac{1}{2}\pi-i$ correspond to $x_1(i)$,

$\theta_2=\frac{1}{2}\pi+i$ correspond to $x_2(i)$,

$\theta_3=\frac{3}{4}\pi$ correspond to x_3,

$\theta_4=\pi-i$ correspond to $x_4(i)$.

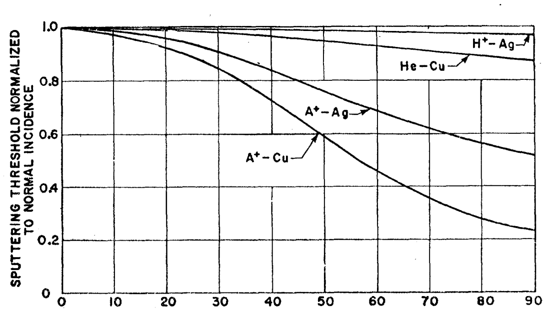

FIG. 8. Polycrystalline thresholds values vs angle of incidence for H^+, and He^+, and Ar^+ on Cu and Ag. The results are normalized to the threshold at 0° angle of incidence.

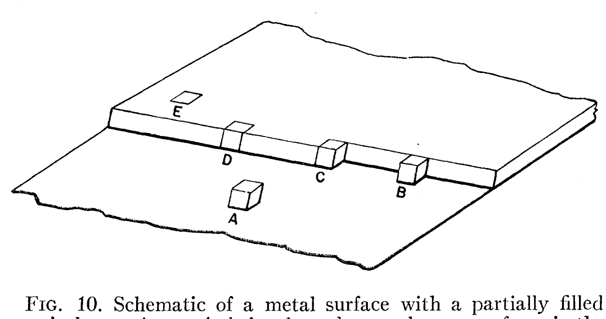

FIG. 10. Schematic of a metal surface with a partially filled atomic layer. Atom A, being bound on only one surface, is the least tightly bound.

TABLE I. Comparison of theoretical and experimental threshold values.

Ion Bombarding	Target	Heat of sublimation[a]	Threshold Theoretical	Threshold Experimental[b]	Crystal structure
			Wehner[c]		
Hg^+	Ag	3.35_7	23.5	120	fcc
	Ni	$[4.41_3]$[d]	18.4	70	fcc
	Cu	3.53_5	14.1	50	fcc
	Rh	$[5.98_6]$[d]	19.5	70	fcc
	Pd	$[4.03_4]$[d]	13.0	50	fcc
	Ag	2.84_5	9.13	40	fcc
	Pt	5.60_8	16.4	70	fcc
	Au	3.90_5	11.4	40	fcc
	Pb	2.30_4	5.94	20	fcc
	Th	{7.07}[e]	20.5	120	fcc
	V	5.28_7	23.9	120	bcc
	Cr	4.03_3	18.0	60	bcc
	Fe	4.12_9	18.0	60	bcc
	Nb	$[7.71_7]$[d]	26.0		bcc
	Mo	6.15_9	20.6	80	bcc
	Ta	8.02_3	23.5	120	bcc
	W	(8.80)[f]	25.7	80	bcc
	Ti	4.84_4	8.79	110	hcp
	Co	4.40_2	18.3	80	hcp
	Zr	6.14_1	20.9	120	hcp
	Hf	$[7.37_4]$[d]	21.6	150	hcp
	Si	$[3.91_0]$[d]	21.6	60	dia
	Ge	4.07_7	15.2	40	dia
	U	{9.57}[e]	22.7	70	rhom
			Morgulis and Tischenko[g]		
He^+	Tl^{204}	1.87_4	5.25	11	hcp
	Sb^{124}	{1.74}[e]	3.13	11	rhom
	Ag^{110}	2.84_5	4.55	12	fcc
	Co^{60}	4.40_2	4.40	12.5	hcp
	Zr^{95}	6.14_1	8.60	15	hcp
	Ir^{192}	{5.22}[e]	14.1	16	fcc
	W	(8.80)[f]	22.5,20.5[h]	20	bcc
Ar^+	Zn^{65}	1.36_6	2.24	3	hcp
	Sb^{124}	{1.74}[e]	1.16	3	rhom
	Tc^{204}	1.87_4	1.20	3	hcp
	Ag^{110}	2.84_5	1.62	4	fcc
	Zr^{95}	6.14_1	5.40	7	hcp
	Ir^{192}	{5.22}[e]	3.34	8	fcc
	Ta^{182}	8.02_3	5.12	13	bcc
	W^{185}	(8.80)[f]	5.63	13	bcc
	Co^{60}	4.40_2	9.0	6	hcp
Hg^+	Co^{60}	4.40_2	18.1	7.2,14.4[i]	hcp
			McKeown[j]		
Ar^+	Au	3.90_5	2.50	10	fcc
			Stuart and Wehner[k]		
Ar^+	Cr	4.03_3	11.8	15	bcc
Hg^+	Cr	4.03_3	18.0	15	bcc

[a] Heats of sublimation from C. J. Smithells, *Metals Reference Book* (Butterworths Scientific Publications, Ltd., London, 1955), 2nd ed., unless otherwise noted.
[b] Lower experimental limit is assumed.
[c] Experimental values are "cut-in" thresholds.
[d] [ ] Value from Langberg dissertation, Princeton University, 1956 (unpublished).
[e] { } Value from F. Seitz, *Modern Theory of Solids* (McGraw-Hill Book Company, Inc., New York, 1940).
[f] ( ) Approximate value.
[g] See reference 1.
[h] Value computed from 1.6-ev binding energy.
[i] Hg^{++} ions.
[j] See reference 3.
[k] See reference 2

Case A. $0 \leq i \leq \pi/4$

By using the integrals and definitions developed above, we write down the polycrystalline sputtering threshold for "small" angles and $\mu < 1$, as

$$\bar{E}_S^{<}(i) = \frac{2}{\pi} \frac{H_{hkl}}{T_m} \{2I(x_3) - I(x_1) - I(x_2)\}. \tag{31}$$

Case B. $\frac{1}{4}\pi \leq i \leq \frac{1}{2}\pi$

The "large" angle threshold formula for $\mu < 1$ is

$$\bar{E}_L^{<}(i) = \frac{2}{\pi} \frac{H_{hkl}}{T_m} \{I(x_4) - I(x_1)\}. \tag{32}$$

Figure 8 is a normalized evaluation of these expres-

sions for helium and argon sputtering copper and silver. Figure 9 illustrates a plot of $E_t^{<}/H_{hkl}$ for mass ratios less than 1, at normal incidence.

COMPARISON WITH EXPERIMENT AND CONCLUSIONS

Because of the dependence upon H_{hkl}, it is very difficult to make a direct comparison between the preceding results and experiment. In the polycrystalline case there is a great temptation to set H_{hkl} equal to the atomic heat of sublimation, but we shall see that this assumption has no basis in either theory or experiment.

Figure 10 shows a schematic drawing of a metal surface with a partially filled atomic layer. Atom A, which rests upon a filled plane is least tightly bound; B, having contact with two surfaces is next; and so on through atom E, which contacts 5 surfaces. Our primary concern is with the liberation of atoms from state A, B, or C. The bombardment process introduces vacancies at the surface; therefore, we expect a considerable enhancement of the usual number of atoms in these states. We note that the theory does not depend upon this surface activation except through the numerical value chosen for H_{hkl}, but in many respects this bombardment activation is equivalent to the first stage of the momentum transfer model proposed by Kingdon and Langmuir,[17] many years ago.

An alternative picture of this activation can be made in purely energetic terms if we assume that the states A, B, and C are at least metastable. Here we postulate that some earlier bombarding atom, whether it actually produced a sputtering event or not, supplied enough energy to activate a surface atom from an energy state corresponding to the pictorial state E into an energy state corresponding to A, B, or C. If the new state is metastable, a subsequent event can then sputter the atom.

Only for tungsten do we have direct experimental measurements of H_{hkl} for an atom in state A. Sokol'skaia[18] reports a value of 1.6 ev, with a heat of sublimation of 8.9 ev, which confirms earlier estimates by Stranski and Suhrmann[19] and Müller.[20] To facilitate comparison of our results with experimental data, we shall arbitrarily assume that $H_{hkl}=\frac{1}{5}H_s$, where H_s is the atomic heat of sublimation. This is equivalent to assigning two atomic bonds per "direction" in the fcc case. Numbers obtained in this fashion may be in error by as much as a factor of two, but probably will not be high. Polycrystalline thresholds for a number of metal-ion combinations are shown in Table I. The theoretical values are consistently lower than Wehner's "cut-in thresholds,"[6] comparable to or lower than the results of Wehner and Stuart[2] and McKeown,[3] and definitely higher than the mercury-cobalt results reported by Morgulis and Tishchenko.[1(a)] However, a careful analysis of the Morgulis and Tishchenko experimental setup, insofar as such an analysis is possible from the published description, indicates that there is considerable probability of an admixture of Hg^{++} ions in the discharge. In terms of Hg^{++} the reported threshold of $\sim$16 ev, which is quite good agreement with the theoretical prediction if we consider the uncertainty in H_{hkl} and recall that cobalt is hexagonal close packed so that the polycrystalline averaging procedure is no longer valid. The more comprehensive data reported by Morgulis and Tishchenko[1(b)] are also higher than the theoretical thresholds for all metal-ion pairs except those involving cobalt. For tungsten, where the binding energy is experimentally known, there is excellent agreement between theory and experiment for helium bombardment where the theory is clear-cut, and somewhat poorer agreement with argon where the theoretical model is more ambiguous.

We conclude that a simple collision model coupled with the chaining mechanism is sufficient to explain presently reported experimental values, but we must reiterate that there is still no direct evidence that a true experimental threshold actually exists.

ACKNOWLEDGMENT

One of the authors (DEH) wishes to acknowledge several conversations with M. T. Robinson of Oak Ridge National Laboratory which helped to refine the model presented in this paper.

[17] K. Kingdon and I. Langmuir, Phys. Rev. **22**, 148 (1923).

[18] I. L. Sokol'skaia, Bull. Acad. Sci. USSR, Phys. Ser. **20**, 10, 1044 (1956).

[19] I. N. S. Stranski and R. Suhrmann, Ann. Physik **1**, 153 (1947).

[20] E. W. Müller, Z. Physik **126**, 643 (1949).